Preparation and Characterisation of $(SeNSNS)_n(AsF_6)_2$ containing the 'Electron-rich Aromatic' 6π $SeNSNS^{2+}$ ($n = 1$) and 7π $SeNSNS^{\bullet+}$ ($n = 2$)‡

Edward G. Awere,[a] Wendell V. F. Brooks,[a] Jack Passmore,*[,a] Peter S. White,*[,†,a] Xiaoping Sun[a] and T. Stanley Cameron*[,b]

[a] *Department of Chemistry, University of New Brunswick, Fredericton, New Brunswick E3B 6E2, Canada*
[b] *Department of Chemistry, Dalhouise University, Halifax, Nova Scotia B3H 4J3, Canada*

Attempted syntheses of $SeNSAsF_6$ from the reactions of $SNAsF_6$ with $Se_8(AsF_6)_2$ (4:1) or Se (1:1) gave $(SeNSNS)_n(AsF_6)_2$ ($n = 1$ and 2), $Se_4(AsF_6)_2$ and trace amounts of $SeNSNSe(AsF_6)_2$ and $(Se/SNSNSe)_2(AsF_6)_2$. The formation of $(SeNSNS)_n(AsF_6)_2$ ($n = 1$ and 2) as the major product is consistent with generation of a $SeNS^+$ intermediate which undergoes a concerted symmetry-allowed cycloaddition reaction with SN^+ to give $SeNSNS^{2+}$. The crystal structure of $SeNSNS(AsF_6)_2$ consists of disordered $SeNSNS^{2+}$ cations and AsF_6^- anions, that of $(SeNSNS)_2(AsF_6)_2$ consists of AsF_6^- anions and two independent disordered $SeNSNS^{\bullet+}$ radical cations weakly linked into a non-centrosymmetric dimer by two long Se···S bonds [3.12(4), 3.09(2); 3.32(5), 3.16(6) Å]. The structure of $(Se/SNSNSe)_2(AsF_6)_2$ contains a 50:50 mixture of disordered $SeNSNSe^{\bullet+}$ and $SeNSNS^{\bullet+}$ radical cations joined by two long Se/S···Se bonds [3.077(3), 3.138(3) Å]. There are significant interionic interactions in all the salts. The ^{77}Se [−60 °C, δ(Me_2Se) = 2422.4, $\nu_{\frac{1}{2}}$ = 10.4 Hz] and ^{14}N NMR [room temperature (r.t.), δ($MeNO_2$) = 68.9, $\nu_{\frac{1}{2}}$ = 446 Hz] spectra of $SeNSNS^{2+}$ are consistent with a delocalised 6π ring structure. The $SeNSNS^{2+}$ cation readily reacts with CCl_3F to give $ClSeNSNSAsF_6$ the identity of which was confirmed by the determination of its crystal structure. The ESR spectrum of $SeNSNS^{\bullet+}$ in SO_2 solution at r.t. (g = 2.026, broad) and the spectrum of powdered $SeNSNS^{\bullet+}$ in frozen SO_2 at −160 °C were similar to but not identical with those of $SeNSeNSe^{\bullet+}$ $SeNSNSe^{\bullet+}$ and $SNSNS^{\bullet+}$ indicative of a planar 7π system.

We have recently reported[1] an efficient high-yield synthesis of $SNSAsF_6$ by the reactions described by equations (1) and (2) and shown that the compound has an extensive chemistry.[2] An alternative but lower-yield route is described by equation (3).[1] These results motivated us to attempt the synthesis of the related $SeNSAsF_6$ by the analogous routes described by equations (4)–(6), and by the reaction of $SNAsF_6$ with $Se_8(AsF_6)_2$ (4:1 ratio) as shown in equation (7). The results are reported below.

$$\tfrac{1}{2}S_8 + S_4N_4 + 6AsF_5 \xrightarrow{\text{trace } Br_2} 4SNSAsF_6 + 2AsF_3 \quad (1)$$

$$SNAsF_6 + \tfrac{1}{8}S_8 \longrightarrow SNSAsF_6 \quad (2)$$

$$2S_4(AsF_6)_2 + S_4N_4 \longrightarrow 4SNSAsF_6 + \tfrac{1}{2}S_8 \quad (3)$$

$$4Se + S_4N_4 + 6AsF_5 \xrightarrow{\text{trace } Br_2} 4SeNSAsF_6 + 2AsF_3 \quad (4)$$

$$SNAsF_6 + Se \longrightarrow SeNSAsF_6 \quad (5)$$

$$2Se_4(AsF_6)_2 + S_4N_4 \longrightarrow 4SeNSAsF_6 + 4Se \quad (6)$$

$$4SNAsF_6 + Se_8(AsF_6)_2 \longrightarrow 4SeNSAsF_6 + Se_4(AsF_6)_2 \quad (7)$$

† *Present address:* Department of Chemistry, The University of North Carolina at Chapel Hill, Chapel Hill, NC 27599-3290, USA.
‡ *Supplementary data available:* see Instructions for Authors, *J. Chem. Soc., Dalton Trans.*, 1993, Issue 1, pp. xxiii–xxviii.

Experimental

General Procedures and Reagents.—The apparatus, chemicals, general techniques and spectrometers used in this work were the same as described in refs. 1 and 3. Raman, IR, MS, ESR, ^{14}N and ^{77}Se NMR samples were prepared and spectra recorded as described in ref. 3. The NMR acquisition parameters were the same as previously reported.[1,3] Chemical shifts were externally referenced at room temperature (r.t.) to neat $MeNO_2$ (^{14}N) or neat Me_2Se (^{77}Se) with the high-frequency direction positive.

Selenium (BDH, 99%) was vacuum dried. The compounds $SNAsF_6$,[4] $Se_4(AsF_6)_2$,[5,6] $Se_8(AsF_6)_2$,[7] S_4N_4,[8] $AgAsF_6$[4] and $Cl_2SeNSNS$[9] were prepared by published methods. Known compounds in the product were identified as follows: SN^+ (^{14}N NMR),[1] Se_4^{2+} (^{77}Se NMR,[5a] Raman[5b]) and Se_8^{2+} (^{77}Se NMR spectroscopy).[5c]

Attempted Preparations of $SeNSAsF_6$ *leading to* $(SeNSNS)_2(AsF_6)_2$ ($n = 1$ *and* 2).—*Reaction of* $SNAsF_6$ *with selenium* (1:1 *ratio*). Selenium (0.293 g, 3.71 mmol) and $SNAsF_6$ (0.880 g, 3.75 mmol) were stirred in SO_2 (10.54 g) in a two-bulb vessel to produce a green solution at r.t. and a red-brown solution over a yellow solid after 6 h. After 4 d the solution was filtered into the second bulb and the yellow solid was washed three times with SO_2 (*ca.* 1 cm^3). The solvent was then slowly condensed into the first bulb which was cooled with dripping cold tap-water (*ca.* 10 °C). After 3 d the solvent was removed giving a yellow powder, $Se_4(AsF_6)_2$ (0.354 g; Raman, ^{77}Se NMR spectra), as the

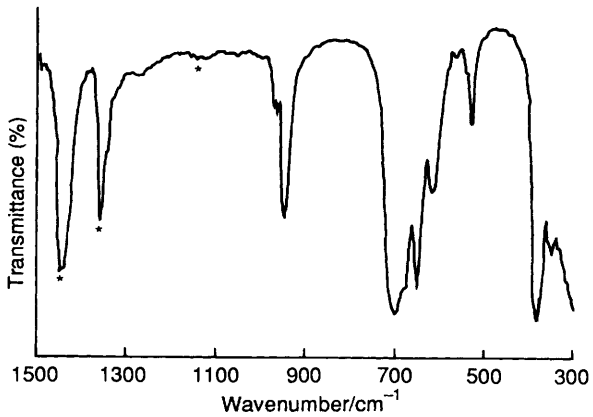

Fig. 1 Infrared spectrum of $(\overline{SeNSNS})_2(AsF_6)_2$. Nujol peaks indicated by asterisks

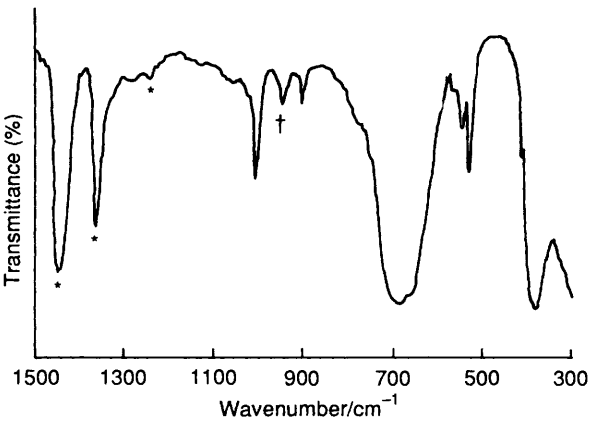

Fig. 2 Infrared spectrum of $\overline{SeNSNS}(AsF_6)_2$. Nujol peaks indicated by asterisks, $\overline{SeNSNSe}(AsF_6)_2$ peaks by a dagger

less-soluble product and black crystals (0.791 g) containing small amounts of yellow microcrystalline crystals [$\overline{SeNSNS}$-$(AsF_6)_2$; IR spectrum, see below] as the more soluble fraction. Several of the black crystals were mechanically selected under the microscope and were identified as $(\overline{SeNSNS})_2(AsF_6)_2$ by X-ray analysis (see below). The IR spectrum of $(\overline{SeNSNS})_2$-$(AsF_6)_2$ in Nujol is shown in Fig. 1: 989 (sh), 982 (sh), 963s, 713vs (AsF_6^-), 687 (sh) (AsF_6^-), 665s, 634s, 585w, 558 (sh), 547s, 395s (AsF_6^-) and 365m (AsF_6^-) cm^{-1}.

Reaction of $SNAsF_6$ *with selenium followed by oxidation by* AsF_5 *with a trace of* Br_2. Selenium (0.990 g, 12.53 mmol) and a 10% deficit of $SNAsF_6$ (2.614 g, 11.12 mmol) (relative to a 1:1 ratio) were stirred in SO_2 (11.52 g) in a two-bulb vessel to give a red-brown solution over a yellow solid after 1 week. The less-soluble yellow solid [1.04 g, $Se_4(AsF_6)_2$; Raman spectrum] was separated from the red-brown solution into which AsF_5 (6.61 g, 38.9 mmol) and a trace of Br_2 were successively condensed; the solution changed to transparent yellow after 2 h. Crystals were grown over a period of 3 d as described above and volatile materials were removed to give yellow crystals (3.08 g) containing small amounts of yellow powder. The yellow crystals were identified as $\overline{SeNSNS}(AsF_6)_2$ by X-ray analysis (see below). The IR spectrum of $\overline{SeNSNS}(AsF_6)_2$ is shown in Fig. 2, the FT Raman spectrum in liquid AsF_3 in Fig. 3 and the vibrational data are listed in Table 1.

In a similar reaction, $SNAsF_6$ (0.265 g, 1.13 mmol) and Se (0.089 g, 1.13 mmol) were allowed to react in SO_2 (3.56 g) in a 10 mm thick-walled NMR tube. After 8 d the ^{14}N NMR spectrum

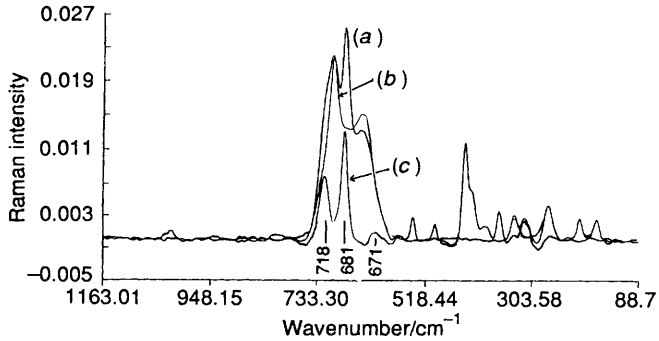

Fig. 3 Fourier-transform Raman spectrum at r.t. of $\overline{SeNSNS}(AsF_6)_2$ in liquid AsF_3 (*a*), neat liquid AsF_3 (*b*), and $\overline{SeNSNS}(AsF_6)_2$ after subtraction of the peaks due to the solvent AsF_3 (*c*)

showed unreacted SN^+ (*ca.* 10 mmol%). The solution was heated at 40 °C for 5 additional days but the amount of unreacted SN^+ was essentially the same after this period (^{14}N NMR). Arsenic pentafluoride (0.95 g, 5.6 mmol) and a trace of Br_2 were successively added giving a transparent yellow solution without any solid materials. The ^{77}Se NMR spectrum (r.t.) acquired after 18 h showed a weak peak at δ 2421.0, $\nu_{\frac{1}{2}}$ = 41.7 Hz and a peak attributable to Se_4^{2+}. At −60 °C a strong peak at δ 2422.4, $\nu_{\frac{1}{2}}$ = 10.4 Hz and peaks attributable to Se_4^{2+} and $\overline{SeNSNSe}^{2+}$ [3] (trace) were observed in the integration ratio *ca.* 14:34:1. We have assigned the peak at δ 2422.4 (−60 °C) [2421.0 (r.t.)] to $\overline{SeNSNS}^{2+}$. We estimated from the ^{77}Se NMR (−60 °C) and weight data that the original product contained *ca.* 40% Se_4^{2+}, 30% $\overline{SeNSNS}^{2+}$ and 30% $\overline{SeNSNS}^{\bullet+}$ (in mmol%). The trace amount of $\overline{SeNSNSe}^{2+}$ was ignored in the estimate. Volatile materials were removed and the resulting yellow solid was subjected to dynamic vacuum (*ca.* 4 h) until constant weight (0.384 g).

In an attempt to isolate pure $\overline{SeNSNS}(AsF_6)_2$, slightly impure $(\overline{SeNSNS})_2(AsF_6)_2$ (0.855 g) was oxidised by AsF_5 (2.45 g, 14.4 mmol) with a trace of Br_2 in SO_2 (7.84 g) in a two-bulb vessel. The more-soluble product (0.549 g) was separated from the purer less-soluble fraction (0.567 g) and the latter was washed three times with the solvent (*ca.* 2 cm^3) after which volatile materials were removed. The ^{77}Se NMR spectrum (−60 °C) of the purer (less-soluble) fraction in SO_2–AsF_5 showed mainly the presence of $\overline{SeNSNS}^{2+}$, small amounts of $\overline{SeNSNSe}^{2+}$ [3] and a peak attributable to Se_4^{2+} in the integration ratio of 63:9:5. The ^{14}N NMR spectrum (r.t.) showed a broad peak at δ 68.9, $\nu_{\frac{1}{2}}$ = 446 Hz ($\overline{SeNSNS}^{2+}$), SN^+ and SNS^+ in the integration ratio of 64:7:1. The more (less-pure)-soluble fraction contained the same species but in a different distribution [^{77}Se NMR (−60 °C) $\overline{SeNSNS}^{2+}$:Se_4^{2+}:$\overline{SeNSNSe}^{2+}$ = 40:29:4; ^{14}N NMR (r.t.) $\overline{SeNSNS}^{2+}$:SN^+:SNS^+ = 46:35:2].

Reaction of $SNAsF_6$ *with* $Se_8(AsF_6)_2$ (4:1 *ratio*). The compounds $SNAsF_6$ (0.725 g, 3.08 mmol) and $Se_8(AsF_6)_2$ (0.768 g, 0.761 mmol) were stirred in SO_2 (7.26 g) in a two-bulb vessel. The colour changes, method of crystal growth and product work-up were as described above. The yellow powder in the less-pure fraction was identified as $Se_4(AsF_6)_2$ (0.454 g; Raman, ^{77}Se NMR spectra) and the more-soluble fraction (0.986 g) contained a mixture of yellow and black crystals which were identified as $\overline{SeNSNS}(AsF_6)_2$ and $(\overline{SeNSNS})_2(AsF_6)_2$, respectively from their IR spectra. The black crystals were further characterised as $\overline{SeNSNS}^{\bullet+}$ by a detailed analysis of the powder ESR spectrum in frozen SO_2.[11] We independently obtained an ESR spectrum of $(\overline{SeNSNS})_2(AsF_6)_2$ (*ca.* 4.8×10^{-3} mol dm^{-3}) in SO_2 at r.t. (g = 2.026, broad) and a

powder ESR spectrum in frozen SO_2 at −160 °C which were identical to those obtained in ref. 10. A trace of $\overline{SNSNS}^{\bullet+}$ (quintet, $g = 2.011$) was also observed in some of the ESR spectra obtained in SO_2 solution at r.t. One yellow and one black crystal were characterised by X-ray crystallography as $\overline{SeNSNSe}(AsF_6)_2$[3] and $(Se/\overline{SNSNSe})_2(AsF_6)_2$, respectively, although both compounds were formed in trace amounts (^{77}Se NMR spectroscopy, see below).

A similar reaction of $SNAsF_6$ (0.115 g, 0.488 mmol) with $Se_8(AsF_6)_2$ (0.123 g, 0.122 mmol) in SO_2 (3.40 g) in a 10 mm NMR tube followed by oxidation by AsF_5 (1.3 g, 7.6 mmol) with traces of Br_2 was carried out as described for the reaction of $SNAsF_6$ with Se. After 8 d the amount of unreacted SN^+ was estimated as *ca.* 15 mmol% (^{14}N NMR spectroscopy). The ^{77}Se NMR (−60 °C) and weight data gave the original distribution of products as *ca.* 60% Se_4^{2+}, 20% $\overline{SeNSNS}^{2+}$ and 20% $\overline{SeNSNS}^{\bullet+}$ (in mmol%). A trace of $\overline{SeNSNSe}^{2+}$ was ignored in the estimate. Volatile materials were removed and the resulting yellow solid (0.284 g) contained mainly $\overline{SeNSNS}(AsF_6)_2$ (IR), $Se_4(AsF_6)_2$ (^{77}Se NMR spectroscopy) and a weak band at 962 cm^{-1} attributable to $\overline{SeNSNSe}(AsF_6)_2$.[3]

Reaction of Se, S_4N_4 *and* AsF_5 *with a trace of* Br_2. Arsenic pentafluoride (1.186 g, 6.98 mmol) and a trace of Br_2 were successively condensed at −196 °C onto a mixture of S_4N_4 (0.188 g, 1.03 mmol) and Se (0.322 g, 4.08 mmol) in SO_2 (3.63 g) in a 10 mm thick-walled NMR tube. An intense green solution formed at r.t. which became transparent yellow-brown after 25 min. The ^{77}Se NMR spectrum at r.t. showed a Se_4^{2+} peak, and at −70 °C a precipitate formed and only a weak peak attributable to $\overline{SeNSNSe}^{2+}$[3] was observed. Volatile materials were removed and the resulting yellow solid (1.66 g) was partially redissolved in fresh SO_2 (3.97 g) allowing separation of the less-soluble product $Se_4(AsF_6)_2$. The more-soluble fraction contained Se_4^{2+} (^{77}Se NMR), $\overline{SeNSNSe}^{2+}$[3] and $\overline{SeNSNS}^{2+}$ (IR, ^{77}Se NMR spectra), and trace amounts of SN^+ (^{14}N NMR), $SNSAsF_6$, $\overline{SNSNS}(AsF_6)_2$ and $F\overline{SNSNS}AsF_6$ (IR spectra). On removal of volatile materials $SNAsF_6$ and $SNSAsF_6$ give $\overline{SNSNS}(AsF_6)_2$ which on grinding abstracts a fluoride ion from AsF_6^- to give $F\overline{SNSNS}AsF_6$ and AsF_5.

Reaction of $Se_4(AsF_6)_2$ *with* S_4N_4 (2:1 *ratio*). The compounds $Se_4(AsF_6)_2$ (0.787 g, 1.13 mmol) and S_4N_4 (0.101 g, 0.55 mmol) were stirred in SO_2 (6.04 g) in a two-bulb vessel to produce an intense green solution with a yellow tint at r.t., and a brown solid after 6 h. The solution was filtered into the empty bulb after 18 h and the brown solid was washed once with solvent (*ca.* 1 cm^3). The less-soluble brown solid (0.182 g) contained $(\overline{SeNSNSe})_2(AsF_6)_2$ (IR spectrum) and the more-soluble product consisted of a mixture of yellow and greenish black solids containing $Se_n(AsF_6)_2$ [$n = 4$ or 8; ^{77}Se NMR (−70 °C)], SN^+ (^{14}N NMR) and $\overline{SeNSNS}^{\bullet+}$ (ESR spectrum).

Some Properties of $(\overline{SeNSNS})_n(AsF_6)_2$ ($n = 1$ *and* 2).—Crystals of $\overline{SeNSNS}(AsF_6)_2$ are yellow and moderately soluble in liquid SO_2 but dissolve readily in a mixture of SO_2–AsF_5 at *ca.* −40 °C, increasing in solubility as the temperature is lowered. It is soluble in liquid AsF_3, very sensitive to traces of moist air, and rapidly acquires a brown coating. The ^{77}Se NMR spectrum of a fresh solution of $\overline{SeNSNS}(AsF_6)_2$ prepared *in situ* with an excess of AsF_5 showed a broad weak peak at r.t. (δ 2421.0, *cf* 2422.4 at −70 °C). If the compound is manipulated inside the dry-box and then redissolved in SO_2 a peak is observed only at low temperature (*e.g.* −70 °C) which shows that it is very hygroscopic. The $\overline{SeNSNS}(AsF_6)_2$ does not readily abstract a fluoride ion from AsF_6^- to form $F\overline{SeNSNS}^+$ on grinding or on prolonged subjection to dynamic vacuum (IR spectrum) in contrast to $\overline{SNSNS}^{2+}$ in $\overline{SNSNS}(AsF_6)_2$.[12] It readily reacts with CCl_3F to give $Cl\overline{SeNSNS}AsF_6$ and the volatile AsF_5 and CCl_2F_2 (IR spectra, see below), and its mass spectrum shows peaks attributable to fragmentation of AsF_5 (*i.e.* AsF_4^+ to As^+) as the most abundant species. This shows that the first process involved the transfer of a fluoride ion from AsF_6^- to $\overline{SeNSNS}^{2+}$ to form the solid $F\overline{SeNSNS}AsF_6$ and the volatile AsF_5.

Crystals of $(\overline{SeNSNS})_2(AsF_6)_2$ are black in the crystalline state and brown in the powdered form. The compound is moderately soluble in liquid SO_2 and dissociates in solution to give $\overline{SeNSNS}^{\bullet+}$ radicals (ESR)[11] which do not react with CCl_3F (IR spectrum).

Preparation of $Cl\overline{SeNSNS}AsF_6$.—The compound $Cl\overline{SeNSNS}AsF_6$ was formed in an attempt to separate $Se_4(AsF_6)_2$ from the products of the reaction of $SNAsF_6$ (1.515 g, 6.45 mmol) and $Se_8(AsF_6)_2$ (1.63 g, 1.61 mmol) in SO_2 (9.56 g). When the reaction was complete CCl_3F (total 4.2 g) was added in aliquots to the solution until a small amount of black crystals formed on the yellow solid. The solution was then filtered into the second bulb, the yellow solid was washed twice with solvent (*ca.* 1 cm^3) and crystals were grown as described above over a period of 3 d. The solvent was removed to give a yellow solid [2.0 g, $Se_4(AsF_6)_2$ (Raman, ^{77}Se NMR spectra)] as the less-soluble product, and a mixture (1.095 g) of yellow and black [$(\overline{SeNSNS})_2(AsF_6)_2$, IR spectrum] crystals as the more-soluble portion. The yellow crystals were identified as $Cl\overline{SeNSNS}AsF_6$ by a complete determination of the crystal structure (see below). IR (Nujol mull) data for $Cl\overline{SeNSNS}AsF_6$: 918vs, 813vw (AsF_6^-), 746 (sh), 698vs (AsF_6^-), 677 (sh), 648 (sh), 628w (sh), 568m, 548m, 395s (AsF_6^-), 361m and 348m cm^{-1}.

Normal Coordinate Analyses.—We hoped that a determination of force constants from IR and Raman spectra would provide additional information about bond strengths. The seven in-plane vibrational modes are insufficient to determine the diagonal force constants (five stretching and five bending) so we tried to use stretching force constants from $\overline{SNSNS}^{2+}$ and $\overline{SeNSNSe}^{2+}$ adjusted according to Badger's rule.[13] This gave very unsatisfactory results because of the short N–S distance (1.457 Å) which calls for a large force constant (> 6.0 N m^{-1}) giving one vibrational mode at a much higher wavenumber (> 1200 cm^{-1}) than observed. For vibrational calculations, we therefore used a structure estimated from those of $\overline{SNSNS}^{2+}$,[12] $\overline{SeNSNSe}^{2+}$[3] and $\overline{SeNSeNSe}^{2+}$.[14] Some assumptions were made to reduce the number of variables. The results are given in Tables 2 and 3. The stretching constants are comparable to those of the three related species. The force constants (and assumed bond strengths) can account for the observed frequencies.

X-Ray Crystallographic Analyses.—$(\overline{SeNSNS})_2(AsF_6)_2$. The data were collected at 291 K using a CAD-4 four-circle diffractometer with an ω–2θ scan. After reduction to a standard scale[15] and application of Lorentz polarisation and absorption[16] corrections, the positions of the As, S and Se atoms were determined with the use of SHELXS[17] and those of the remaining atoms from subsequent Fourier syntheses. The structure was refined by large-block least squares which converged at $R = 0.0457$ with anisotropic thermal parameters for all atoms. In the structure both cations are disordered with the –N–Se–S–N– fragment in the alternative –N–S–Se–N– position (*i.e.* the ring can be flipped over with just the Se and S atoms changing places). The structure was refined (SHELX 76)[18] with the N–S, N–Se and Se–S distances in this fragment each constrained to be equal in both rings and in both

disordered arrangements. The occupation of the two disordered arrangements was also refined and this converged to a value of 0.69:0.31 for ring 1 and 0.65:0.35 for ring 2. These values are close to a ratio of 2:1 and leave a suspicion that the disorder may be derived from a multiple of one of the cell length(s). A detailed photographic study failed to find any convincing evidence of such a multiple but, given the structure, the evidence could be very faint. One of the AsF_6^- anions [As(1)] shows considerable thermal motion. Attempts were made to fit a disordered model to this motion but invariably produced unreasonable thermal parameters. It seems likely that the ion is librating strongly. This is not an unexpected behaviour and no attempt was made to analyse the motion.

$\overline{SeNSNS}(AsF_6)_2$. The data were collected as described above. After reduction to a standard scale[15] and application of Lorentz and absorption[16] corrections, the positions of all the atoms were derived by comparison with the structure of $\overline{SNSNS}(AsF_6)_2$[12] which is isomorphous. The structure was refined initially with SHELX 76[18] and finally with CRYSTALS.[19] Large-block least squares was used in the refinement which converged at $R = 0.0404$ with anisotropic thermal parameters for all atoms (there are no hydrogen atoms in the structure). The structure belongs to the space group $C2$ where the origin along y is not fixed by symmetry. In the final stages of the refinement the origin was fixed by requiring the sum of all y shifts to be equal to zero. The enantiomer was checked by refining the structure in both possible 'hands' and the parameters reported here gave a drop in R of nearly 2% from 0.065. As in the case of the monocation, the ring is disordered with both the –N–Se–S–N– and –N–S–Se–N– arrangements of the ring present. The S and Se atoms were resolved in the last refinement by refining only the Se–S fragment of the structure with both arrangements of the Se–S fragment present. The two S–Se, N–S and N–Se distances were each restrained[20] to be equal, and although the initial values were set at 2.2, 1.5 and 1.9 Å, respectively, the distances were also allowed to refine. The occupation factors for both arrangements were allowed to refine subject only to the condition that the total occupation sum should be 1.0. The refinement converged with the S and Se atoms on each site clearly resolved and with the occupation for each arrangement in the ratio of 0.51:0.49, essentially equally occupied. There are three unique As atoms in the structure, belonging to an AsF_6^- anion and two As atoms on two-fold axes, which contribute half an AsF_6^- anion each.

While the refinement appears to be successful one concern remains. Clearly the bulk of all the reflections belong to the system cited in the crystal data (see Table 4). However, there are a small number of additional X-ray reflections with small intensities which do not fit this system. These would fit a cell of dimensions $a = 25.12$, $b = 17.12$, $c = 10.616$ Å, $\beta = 93.3°$. There are not enough of them to establish this larger cell firmly, yet there are too many to be lightly ignored. The corresponding $\overline{SNSNS}(SbF_6)_2$ salt has a similar cell with $a = 25.90$, $b = 17.56$ and $c = 10.54$ Å. This is apparently in space group $C222_1$, but it too has a prominent sub-cell with a and b halved. The structure of the SbF_6^- salt has not yet been properly determined. These structures may be just two examples of polytypism, which is not unexpected since they are, after all, just simple binary compounds which often display polytypism (*e.g.* ZnS).[21] The possible lattice ambiguity for the monocation has already been noted which may also be the start of another polytypical family. The possible resolution of the disorder in these AsF_6^- salts will be pursued when the details of the structure of the SbF_6^- salt have been determined. Crystal data and final atomic coordinates for $(\overline{SeNSNS})_2(AsF_6)_2$ and $\overline{SeNSNS}(AsF_6)_2$ are presented in Tables 4 and 5, respectively.

$(Se/\overline{SNSNSe})_2(AsF_6)_2$ *and* $ClSeNSNSAsF_6$. Diffraction intensities were measured at 293 K on an Enraf-Nonius CAD-4 diffractometer equipped with graphite-monochromated Mo-Kα radiation (λ = 0.710 73 Å) using the NRCCAD[22] control program. An ω–2θ scan was used and backgrounds were estimated by extending the scan by 25% on either side of the scan limits. The limits of the peak were then ascertained by profile analysis to provide an improved background correction. Unit-cell parameters for $(Se/\overline{SNSNSe})_2(AsF_6)_2$ and $ClSeNSNSAsF_6$ were obtained by least-squares refinement using the coordinates of 25 (2θ 30–40) and 26 (2θ 30–36°) reflections, respectively, centred using the TRUANG option of NRCCAD, thereby minimising the effects of instrumental and crystal-alignment errors. Lorentz and polarisation factors were applied and absorption corrections for $ClSeNSNSAsF_6$ were made using the empirical routine of Walker and Stuart.[16] No correction was made for absorption of $(Se/\overline{SNSNSe})_2(AsF_6)_2$.

The structures were solved by direct methods and subsequent difference syntheses. Crystal data are summarised in Table 4. Refinement was by full-matrix least squares with weights based on counter statistics. All atoms were refined with anisotropic thermal parameters. Computations were performed using the NRCVAX suite of crystal structure programs.[23] Scattering factors were taken from ref. 24 and were corrected for anomalous dispersion. The final atomic coordinates are given in Table 6.

Additional material available from the Cambridge Crystallographic Data Centre comprises thermal parameters and remaining bond lengths and angles.

Results and Discussion

Attempted Preparations of $SeNSAsF_6$ *leading to* $(\overline{SeNSNS})_n(AsF_6)_2$ (n = 1 *and* 2).—*Reaction of* $SNAsF_6$ *with* Se (1:1 *ratio*) *or* $Se_8(AsF_6)_2$ (4:1 *ratio*). The reactions of $SNAsF_6$ with Se (1:1 ratio) or $Se_8(AsF_6)_2$ (4:1 ratio) which were designed to give $SeNSAsF_6$ did not proceed as envisaged in equations (5) and (7) but instead gave $(\overline{SeNSNS})_n(AsF_6)_2$ (n = 1 and 2) as major products, as well as $Se_4(AsF_6)_2$ (Raman, ^{77}Se NMR spectra) and a trace amount of $\overline{SeNSNSe}(AsF_6)_2$[3] (IR, ^{77}Se NMR spectra). The colour changes of the two reactions were identical and there was no evidence for nitrogen elimination. The ^{14}N NMR spectra of the bulk products of both reactions acquired after 3 d to 1 week showed unreacted SN^+. In two separate experiments the amount of unreacted SN^+ was estimated as *ca.* 10 and 15 mol%, respectively for reactions (5) and (7) (^{14}N NMR spectrum). The amount of unreacted SN^+ was essentially the same (^{14}N NMR spectrum) after heating the solutions at 40 °C for 5 additional days which indicated that the reactions were complete after 1 week.

The reactions may be described by equations (8) and (9) to

$$8SN^+ + 2Se_8^{2+} \longrightarrow 3Se_4^{2+} + 2\overline{SeNSNS}^{2+} + 2\overline{SeNSNS}^{\bullet+} \quad (8)$$

$$8SN^+ + 8Se \longrightarrow Se_4^{2+} + 2\overline{SeNSNS}^{2+} + 2\overline{SeNSNS}^{\bullet+} \quad (9)$$

account for the observed products. However, these equations do not represent the distribution of products as estimated from the ^{77}Se NMR (−60 °C) and weight data acquired after reaction of the bulk products with AsF_5. The reaction of $SNAsF_6$ with Se gave the original distribution of products as *ca.* 30% $(\overline{SeNSNS})_2(AsF_6)_2$, 30% $\overline{SeNSNS}(AsF_6)_2$ and 40% $Se_4(AsF_6)_2$ (in mmol%), while that of $SNAsF_6$ with $Se_8(AsF_6)_2$ gave *ca.* 20% $(\overline{SeNSNS})_2(AsF_6)_2$, 20% $\overline{SeNSNS}(AsF_6)_2$ and 60% $Se_4(AsF_6)_2$. The trace amount of $\overline{SeNSNSe}(AsF_6)_2$ was ignored in both cases for the purpose of estimation. These reactions give predominantly one selenium-containing salt [*i.e.* $(\overline{SeNSNS})_n$-

Table 1 Vibrational data (cm^{-1}) for $\overline{SeNSNS}(AsF_6)_2$ and assignments[a]

IR[b] (Nujol)	Raman Solid[c,d] −196 °C, 5145 Å	Raman AsF_3 Solution[e,d] Fourier-transform	Tentative assignment
1015s	1020vw	1020vw	ν (ring)[f]
	941vw		?
915w	922vw		ν (ring)[f]
	724s	718s	ν (ring)[f]
700vs			ν_3 (AsF_6^-)[g]
	681s (br)	681vs	ν_1 (AsF_6^-)[g]
674 (sh)		671s (sh)	?
582 (sh)			
562m	560s		ν_2 (AsF_6^-)[g]
545m	543s	545w	ν (ring)[f]
		500w	*h*
430 (sh)			?
	440w	440s	ν (ring)[f]
	424w	425 (sh)	ν (ring)[f]
390s			ν_4 (AsF_6^-)[g]
	368w	371w	ν_5 (AsF_6^-)[g]
	324vs	320w	ν (ring)[f]
		268w	*h*
		207w	?
		175w	?

v = Very, s = strong, m = medium, w = weak, sh = shoulder, br = broad.

[a] The assignments given are based on a normal coordinate analysis of $\overline{SeNSNS}^{2+}$ (see Tables 2 and 3). [b] Crystals were selected under the microscope from the reaction of $SNAsF_6$ with $Se_8(AsF_6)_2$ (4:1 ratio). The IR spectrum obtained was identical to those from the reaction of $SNAsF_6$ with Se (1:1) and from the oxidation of $Cl\overline{SeNSNS}AsF_6$ with an excess of AsF_5. [c] The sample decomposes in the Raman beam (5145 Å) at r.t. [d] From the oxidation of $Cl\overline{SeNSNS}AsF_6$ with an excess of AsF_5. Similar to Fourier-transform Raman spectrum of the product made by the reaction of $SNAsF_6$ with elemental selenium [giving $(\overline{SeNSNS})_2(AsF_6)_2$] followed by oxidation with AsF_5, except that the latter material also contained some $\overline{SeNSNSe}(AsF_6)_2$. [e] Peaks due to AsF_3 are not included. [f] Exact description of the vibrations are given in Tables 2 and 3. [g] By comparison with AsF_6^- salts, ref. 10. [h] $\overline{SeNSNSe}^{2+}$ [3] impurity.

$(AsF_6)_2$, n = 1 or 2]* which suggests that they proceed by a simple mechanism (see below). In contrast, the reaction of S_4N_4 with $Se_4(AsF_6)_2$ (1:1 ratio) gives mainly a mixture of $(\overline{SeNSNS})_2(AsF_6)_2$ (*ca.* 30 mmol%) and $(\overline{SeNSNSe})_2(AsF_6)_2$ (*ca.* 60 mmol%)[3] which indicates that the reaction pathway may be more complex than those described above.

The reaction of SN^+ with selenium (1:1 ratio) or with Se_8^{2+} (4:1 ratio) may proceed by abstraction of a selenium atom to give $SeNS^+$ [equation (10)] by a route similar to that proposed

$$4SN^+ + Se_8^{2+} \longrightarrow 4SeNS^+ + Se_4^{2+} \quad (10)$$

$$4SeNS^+ + 4SN^+ \longrightarrow 4\overline{SeNSNS}^{2+} \quad (11)$$

$$2\overline{SeNSNS}^{2+} + Se_8^{2+} \longrightarrow 2Se_4^{2+} + 2\overline{SeNSNS}^{\bullet+} \quad (12)$$

for the reaction of SN^+ and S_8.[1] The $SeNS^+$ may then be trapped by SN^+ to give $\overline{SNSNSe}^{2+}$ [equation (11)] in a symmetry-allowed concerted cycloaddition reaction, with the major interaction in the transition state being between the highest occupied molecular orbital (HOMO) of $SeNS^+$ and the lowest unoccupied orbital (LUMO) of SN^+, *i.e.* $SeNS^+$ is acting as a donor towards the more electrophilic SN^+ (*cf.* the related cycloaddition of SNS^+ and SN^+ [12]). The ion $\overline{SeNSNS}^{2+}$ may then oxidise Se_8^{2+} (or selenium) to give the observed Se_4^{2+} with the formation of $\overline{SeNSNS}^{\bullet+}$ [equation (12)] and thereby compete with the reaction of SN^+ with Se or Se_8^{2+} [equation (10)] and this may account for unreacted SN^+.

The direct reduction of SN^+ gives $S_4N_4^{2+}$ which was not observed in the IR spectra of the products which shows that the direct oxidation of Se or Se_8^{2+} by SN^+ did not occur, *e.g.* SN^+ is reduced by I_2 to give $S_4N_4^{2+}$ and I_5^+ [see ref. 25(*a*)]. We note that the related $\overline{SeNSNSe}^{2+}$ [3] is a powerful oxidising agent, and in fact difficult to prepare completely free of $\overline{SeNSNSe}^{\bullet+}$. We found that a large excess of SN^+ produced $\overline{SeNSNS}^{2+}$ and Se_4^{2+} but not $\overline{SeNSNS}^{\bullet+}$, whereas an excess of Se or Se_8^{2+} gave $\overline{SeNSNS}^{\bullet+}$ but not the dication. These results are consistent with the proposed reaction pathways [see equations (10)–(12)] and also indicate that $\overline{SeNSNS}^{2+}$ retains its ring structure in solution. The reaction of SN^+ with Se or Se_8^{2+} can be contrasted to that of S_8, S_4N_4 and AsF_5 with a trace of Br_2 which gives SNS^+ *via* the $\overline{SNSNS}^{2+}$ intermediate which completely dissociates into SN^+ and SNS^+.[1] Chivers and co-workers[25b] have reported the preparation of $Cl\overline{SeNSNS}$-$AlCl_4$ from the reaction of $SNAlCl_4$ with C_2H_5SeCl or with selenium in CH_2Cl_2. The authors proposed that the $SeNS^+$ cation was generated as an intermediate which reacted with NSCl to give the observed product. However, in the light of our results it is also possible that $SeNS^+$ reacted with SN^+ to give $\overline{SeNSNS}^{2+}$ which abstracted a chloride ion from the $AlCl_4^-$, CH_2Cl_2 or C_2H_5SeCl starting material. The high chloride-ion

* $\overline{SeNSNS}(AsF_6)_2$ was also identified [IR, Raman and NMR spectra (^{77}Se, ^{14}N)] as a product formed on oxidation of $Cl\overline{SeNSNS}AsF_6$ with an excess of AsF_5. However, on reduction with CsN_3 some $Cl\overline{SeNSNS}AsF_6$ was regenerated (IR spectrum). Clearly, further investigations are needed to solve the puzzle. Also see foonote *d* in Table 1.

Table 2 Assumed structure and calculated force constants of $\overline{SeNSNS}^{2+}$

Coordinate	Distance (Å) or angle (°)	Force constant/ N m^{-1}
S^3–N^1[a]	1.59	363
S^3–N^2[a]	1.59	363
N^1–Se^1[b]	1.70	288
N^2–S^2[c]	1.53	416
Se^1–S^2[d]	2.20	212
N^1–S^3–N^2[d]	104.75	110
S^3–N^1–Se^1	122.2	−25
S^3–N^2–S^2	121.3	2
N^1–Se^1–S^2	90.8	64
N^2–S^2–Se^1	100.8	51

[a] Assumed equal, average from $\overline{SNSNS}^{2+}$ and $\overline{SeNSNSe}^{2+}$. [b] From $\overline{SeNSNSe}^{2+}$, ref. 3. [c] From $\overline{SNSNS}^{2+}$, ref. 12. [d] Average from $\overline{SNSNS}^{2+}$ and $\overline{SeNSNSe}^{2+}$.

Table 3 Observed and calculated in-plane wavenumbers (cm^{-1}) of $\overline{SeNSNS}^{2+}$ amd percentage potential-energy distribution (p.e.d.)

Obs.	Calc.	p.e.d. S^3–N^2	N^1–Se^1	N^2–S^3	Se^1–S^2	Bend
1020	1022	30		50		15
922	928	65	25			10
718	709	55		20		25
545	548	35	40	15		10
440	450	10	20		30	35
425	419		20		40	30
300	317			10	15	75

affinity of $\overline{SeNSNS}^{2+}$ implies that the Cl^- salt is not isolable and the $AlCl_4^-$ salt may not be also.

At the early stage of this work crystals of $\overline{SeNSNSe}(AsF_6)_2$ and $(Se/\overline{SNSNSe})_2(AsF_6)_2$ were selected under the microscope from the reaction of $SNAsF_6$ with $Se_8(AsF_6)_2$ and characterised by X-ray analysis and were erroneously ascribed to be the main products.[11] However, in this work we show that these compounds were formed in trace amounts (see below) which shows that selected crystals may not be representative of the bulk products which can only be reliably characterised unambiguously by a combination of various spectroscopic techniques (X-ray, IR, ^{14}N, ^{77}Se NMR and ESR spectroscopy).

The compound $(\overline{SeNSNS})_2(AsF_6)_2$ was identified by IR spectroscopy and a detailed analysis of the g and hyperfine tensors from its powder ESR spectrum in frozen SO_2 at -196 °C[11] and confirmed by its crystal structure. Its identity was also inferred from the ^{77}Se NMR and IR spectra of the product given on oxidation by AsF_5 which showed mainly $\overline{SeNSNS}(AsF_6)_2$, $Se_4(AsF_6)_2$ and trace amounts of $\overline{SeNSNSe}$-$(AsF_6)_2$.[3] The ESR spectrum of $\overline{SeNSNS}^{\bullet+}$ in SO_2 at r.t. (g = 2.026, broad) and the powder spectrum in frozen SO_2 at -160 °C are similar to but not identical with those of the related 7π radicals, $\overline{SeNSNSe}^{\bullet+}$[3] and $\overline{SeNSeNSe}^{\bullet+}$.[14]

The compound $\overline{SeNSNS}(AsF_6)_2$ was identified by IR and Raman spectroscopy with assignments supported by normal coordinate analysis (see Tables 1–3), and its identity was confirmed by its crystal structure (see below). The attempt to separate $Se_4(AsF_6)_2$ from the more-soluble products of the reaction of $SNAsF_6$ with $Se_8(AsF_6)_2$ using a mixture of SO_2 and CCl_3F surprisingly led to the formation of $Cl\overline{SeNSNS}AsF_6$ (X-ray, IR spectrum). This implied that the $\overline{SeNSNS}^{2+}$ cation was present in solution and reacted with CCl_3F. The high halide-ion affinity of $\overline{SeNSNS}^{2+}$ may be due to the localisation of a positive charge on selenium.

We were not able to isolate pure samples of $(\overline{SeNSNS})_n$-$(AsF_6)_2$ (n = 1 or 2) as their solubilities are similar to that of $Se_4(AsF_6)_2$ in liquid SO_2 and to the presence of small amounts of unreacted $SNAsF_6$ (see Experimental section). The reaction of $Se_8(AsF_6)_2$ or Se with a deficit of $SNAsF_6$ (*ca.* 10%) gives $(\overline{SeNSNS})_2(AsF_6)_2$ and $Se_4(AsF_6)_2$ but not $\overline{SeNSNS}(AsF_6)_2$ and when an excess of $SNAsF_6$ (*ca.* 10%) is used the last two compounds are formed. Attempts to separate pure samples of $(\overline{SeNSNS})_n(AsF_6)_2$ (n = 1 or 2) using these reaction conditions have so far been unsuccessful. We also observed that large crystals of $(\overline{SeNSNS})_2(AsF_6)_2$ were formed by slow recrystallisation in liquid SO_2 for *ca.* 5–7 d. It is therefore possible that pure $(\overline{SeNSNS})_2(AsF_6)_2$ might be isolated by washing the non-crystalline $Se_4(AsF_6)_2$ with SO_2 and then subliming out any unreacted $SNAsF_6$ by pumping under dynamic vacuum. Although the reactions of $SNAsF_6$ with $Se_8(AsF_6)_2$ or Se are both convenient routes to $(\overline{SeNSNS})_n(AsF_6)_2$ (n = 1 or 2), we recommend the use of Se since $Se_8(AsF_6)_2$ must be prepared and purified. The compounds $(\overline{SeNSNS})_2(AsF_6)_2$ and $\overline{SeNSNS}$-$(AsF_6)_2$ form black and yellow crystals, respectively while $Se_4(AsF_6)_2$ is a yellow non-crystalline solid. These differences enabled us to select crystals of the first two compounds under the microscope and to obtain their IR and Raman (n = 2) spectra.

Nature of the $\overline{SeNSNS}^{2+}$ *Cation in Solution.*—We have shown that the $\overline{SNSNS}^{2+}$ cation completely dissociates in solution to give SN^+ and SNS^+[12,26] [see equations (13)] and that this process is one of the key steps in the formation of SNS^+ from the reaction of S_8, S_4N_4 and AsF_5 with a trace of Br_2.[1] This motivated us to investigate the nature of the related $\overline{SeNSNSe}^{2+}$[3] and $\overline{SeNSeNSe}^{2+}$[14] in solution and to explore the possibility of preparing simple Se–N cations from them. However, we found that the last two cations retain their ring structures in solution. We therefore envisaged that $\overline{SeNSNS}^{2+}$ (*cf.* $\overline{SNSNS}^{2+}$) would be more likely to dissociate in solution than $\overline{SeNSNSe}^{2+}$[3] and $\overline{SeNSeNSe}^{2+}$[14] [see equations (14)–(16)]. The ^{77}Se NMR chemical shift of $\overline{SeNSNS}^{2+}$ at -60 °C (δ 2422.4, $\nu_{\frac{1}{2}}$ = 10.4 Hz) was essentially the same as that at r.t. (δ 2421, $\nu_{\frac{1}{2}}$ = 41.7 Hz) which implies that the cation is not in equilibrium with other species in solution. The appearance of the resonance due to $\overline{SeNSNS}^{2+}$ at a high frequency is consistent with the dipositive charge and a delocalised 6π system, and the shift to a higher frequency relative to that of $\overline{SeNSNSe}^{2+}$ (δ 2411.7, $\nu_{\frac{1}{2}}$ = 10.2 Hz)[3] is consistent with the replacement of selenium in $\overline{SeNSNSe}^{2+}$ by the more electronegative sulfur. The related 6π $\overline{SeNSeNSe}^{2+}$ (δ 2434.0, $\nu_{\frac{1}{2}}$ = 9.2 Hz)[14] as its AsF_6^- salt also gave a peak at high frequency.

$$\overline{SNSNS}^{2+} \longrightarrow SNS^+ + SN^+ \quad (13)$$

$$\overline{SeNSNSe}^{2+} \not\longrightarrow SeN^+ + SeNS^+ \quad (14)$$

$$\overline{SeNSeNSe}^{2+} \not\longrightarrow SeN^+ + SeNSe^+ \quad (15)$$

$$\overline{SeNSNS}^{2+} \xrightarrow{?} SeNS^+ + SN^+, \text{ or } SNS^+ + SeN^+ \quad (16)$$

The ^{14}N NMR spectrum of slightly impure $\overline{SeNSNS}(AsF_6)_2$ in SO_2–AsF_5 solution showed a broad peak at δ 68.9, $\nu_{\frac{1}{2}}$ = 446 Hz ($\overline{SeNSNS}^{2+}$) and weak peaks attributable to SN^+ and SNS^+. The broad ^{14}N NMR resonance is consistent with a ring structure which precludes extensive dissociation to small cations such as SeN^+ or $SeNS^+$ which would be expected to have relatively sharp peaks. However, it does not rule out the possibility of slight dissociation (*ca.* 5%) to polymeric species [e.g. $\frac{1}{x}(SeN^+)_x$] which would have broad peaks. The ^{14}N NMR results should be interpreted with caution since we could not isolate very pure $\overline{SeNSNS}(AsF_6)_2$ for the NMR study and the sample contained some SN^+ and SNS^+. The Raman spectrum of $\overline{SeNSNS}(AsF_6)_2$ in AsF_3(l) did not show the presence of detectable amount of SN^+ or SNS^+, and no peaks were observed in the region predicted for SeN^+ or $SeNS^+$ (see Fig. 3). Thus the ^{77}Se and ^{14}N NMR data of $\overline{SeNSNS}^{2+}$ and its Raman spectrum in liquid AsF_3 are all consistent with retention of the ring structure in solution. This retention was also inferred from the formation of $\overline{SeNSNS}^{\bullet+}$ as a product, the presence of unreacted SN^+ [see equations (10)–(12) above], and the rapid formation of $Cl\overline{SeNSNS}^+$ on addition of CCl_3F to a solution containing the dication (see above). The enthalpy change for the dissociation of $\overline{SNSNS}^{2+}$ to SN^+ and SNS^+ in solution has been estimated at *ca.* -6 kJ which indicates that the process is only marginally favourable.[12] The retention of the $Se_{3-x}S_xN_2^{2+}$ (x = 0–2) ring structures in solution is therefore consistent with this result since the enthalpy change is expected to be less favourable with successive replacement of sulfur by selenium.

Reaction of Se, S_4N_4 *and* AsF_5 *with a Trace of* Br_2.—The attempt to prepare $\overline{SeNSAsF_6}$ according to equation (4) led to the formation of $\overline{SeNSNSe}(AsF_6)_2$,[3] $Se_4(AsF_6)_2$ and smaller amounts of $SNAsF_6$, $F\overline{SNSNS}AsF_6$ and $\overline{SeNSNS}(AsF_6)_2$.[12] The distribution of these products could not be determined from the ^{77}Se NMR spectrum because a precipitate formed at -70 °C. The analogous sulfur reaction [see equation (1)] proceeds quantitatively to give $SNSAsF_6$.[1] The observed products indicate that the first step of this reaction involves a rapid oxidation[6] of Se by AsF_5 to form $Se_4(AsF_6)_2$ which then

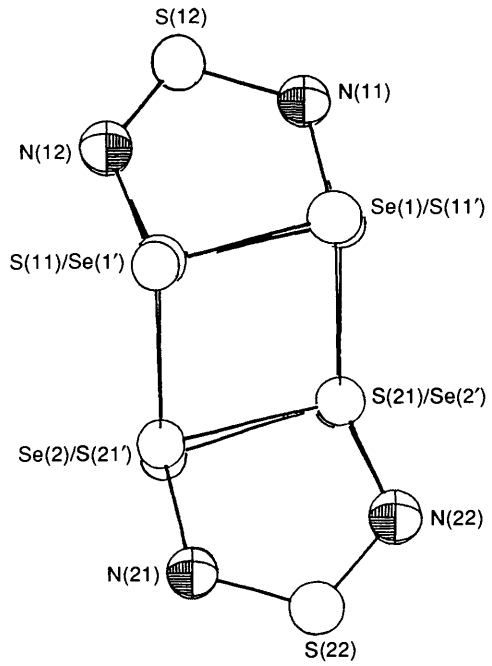

Fig. 4 An ORTEP plot of the disordered $(Se/\overline{SNSNS}/Se^{\bullet+})_2$

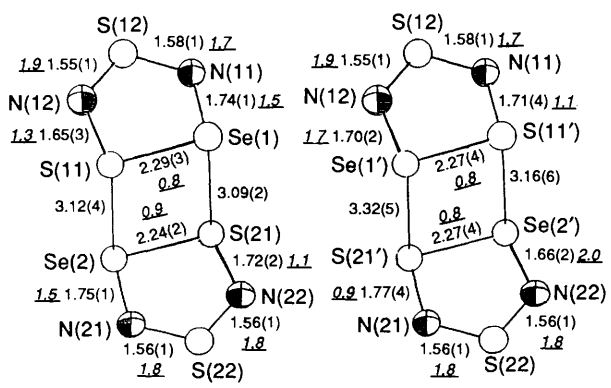

Fig. 5 Bond distances (Å) and calculated bond orders (italics underlined) in the two independent molecules of $(Se/\overline{SNSNS}/Se^{\bullet+})_2$. Occupancy factors: S(11), Se(1) 0.70; Se(1'), S(11') 0.30; Se(2), S(21) 0.65; S(21'), Se(2') 0.35

reacts with S_4N_4 to give $(Se_{3-x}S_xN_2)_2(AsF_6)_2$ (x = 1–3 but largely x = 1 is the key reaction) and Se followed by oxidation with AsF_5 to give $Se_{3-x}S_xN_2(AsF_6)_2$.

Reaction of $Se_4(AsF_6)_2$ *with* S_4N_4 (2:1 *ratio*).—We have described the 1:1 ratio reaction elsewhere.[3] The reaction in a 2:1 ratio was carried out by analogy to the sulfur reaction which gives $SNSAsF_6$ [see equations (3) and (6)]. However, the reaction did not proceed as indicated by equation (6) but instead gave $(\overline{SeNSNSe})_2(AsF_6)_2$,[3] $Se_8(AsF_6)_2$ and $(\overline{SeNSNS})_2(AsF_6)_2$ which indicates that $Se_4(AsF_6)_2$ first reacted with S_4N_4 in a 1:1 ratio to give mainly $(\overline{SeNSNSe})_2(AsF_6)_2$ and selenium and a small amount of $(\overline{SeNSNS})_2(AsF_6)_2$. The selenium then reacted with $Se_4(AsF_6)_2$ to give $Se_8(AsF_6)_2$.

Crystal Structures of $(Se/\overline{SNSNS}/Se)_2(AsF_6)_2$, $Se/\overline{SNSNS}/Se(AsF_6)_2$ *and* $(Se/\overline{SNSNSe})_2(AsF_6)_2$.—The crystal structures are disordered therefore the estimated standard deviations may not represent the actual errors in the bond lengths. That of $(\overline{SeNSNS})_2(AsF_6)_2$ consists of two independent disordered $\overline{SeNSNS}^{\bullet+}$ cations loosely joined into a dimer by two long Se···S bonds, and AsF_6^- anions with significant cation–anion interactions. The structure is more correctly formulated as $(Se/\overline{SNSNS}/Se)_2(AsF_6)_2$. The disorder was modelled by the superimposition of two independent $\overline{SNSNSe}^{\bullet+}$ and $\overline{SeNSNS}^{\bullet+}$ radical cations. The NSN fragment was made to be the same in both arrangements and the two nitrogen atoms and the apical sulfur all have occupancy factors of one. An ORTEP plot[27] of the disordered dimer showing atom numbering is illustrated in Fig. 4. The cations with high Se and S occupancy factors (0.70 and 0.65) form a dimer *via* overlap of their π* singly occupied molecular orbital (SOMO), reminiscent of the dimerisation of related 7π radical cations (see below). Their disordered pairs with low Se and S occupancy factors (0.30 and 0.35) also dimerise in the same way. Thus two independent non-centrosymmetric (with respect to occupancy factors of Se and S) $(\overline{SeNSNS}^{\bullet+})_2$ and $(\overline{SNSNSe}^{\bullet+})_2$ dimers with separate but similar bond distances and angles were obtained. These are shown in Fig. 5 together with their corresponding bond distances and calculated bond orders.* Bond distances within the AsF_6^- anions and the angles within the two dimeric cations are also listed in Table 7.

The structure of $(Se/\overline{SNSNS}/Se^{\bullet+})_2$ is isomorphous (space group $P2_1/n$) with those of $(Se/\overline{SNSNSe}^{\bullet+})_2$ (see below), $(\overline{SeNSNSe}^{\bullet+})_2$[29] and $(\overline{SNSNS}^{\bullet+})_2(AsF_6)_2$[30] (space group $P2_1/c$) but not with $(\overline{SeNSeNSe}^{\bullet+})_2(AsF_6)_2$[14] (space group $P\bar{1}$). The *trans* geometry of $(Se/\overline{SNSNS}/Se^{\bullet+})_2$ and the Se···S distances [3.12(4), 3.09(2), 3.32 (5) and 3.16(6) Å] are similar to those observed in related ring systems which form π*–π* bonds [*e.g.* $(\overline{SNSNS}^{\bullet+})_2(AsF_6)_2$,[30] S···S 2.994(3); $(\overline{SeNSNSe}^{\bullet+})_2(AsF_6)_2$,[29] Se···Se 3.159(2), 3.111(2); $(\overline{SeNSeNSe}^{\bullet+})_2(AsF_6)_2$,[14] Se···Se 2 × 3.123(3), 2 × 3.149(3); and $(Se/\overline{SNSeNSe}^{\bullet+})_2(AsF_6)_2$ (see below), Se/S···Se 3.138(3), 3.077(3) Å], $(C_6H_4Se_3^{\bullet+})_2$[31] [average Se···Se 3.226(4)] and $(Ph_2C_2N_3Se)_2$[32] [Se···Se 2.792(3) Å]. This suggests that the lengths of these weak bonds are independent of the chalcogen.

The crystal structure of $\overline{SeNSNS}(AsF_6)_2$ consists of disordered $\overline{SeNSNS}^{2+}$ cations and AsF_6^- ions with significant interionic interactions. The model used to fit the disorder in $\overline{SeNSNS}^{2+}$ was the same as that described above for the monocation. Both NSeSN and NSSeN arrangements of the ring are present in different unit cells with essentially equal occupancy factors (0.51 and 0.49), but the NSN moiety is the same for both rings. An ORTEP plot of the disordered $\overline{SeNSNS}^{2+}$ (formulated as $Se/\overline{SNSNS}/Se^{2+}$) cation is depicted in Fig. 6, the two independent $\overline{SeNSNS}^{2+}$ cations are shown in Fig. 7, and bond distances and angles are listed in Table 8. The structures of $Se/\overline{SNSNS}/Se(AsF_6)_2$ and $Se_{3-x}S_xN_2^{2+}$ (x = 0, 1 or 3) are isomorphous (space group $C2$) and isostructural.

The bonding in the formally 6π $\overline{SeNSNS}^{2+}$ and 7π $\overline{SeNSNS}^{\bullet+}$ may be described by a simple MO model derived from that of $\overline{SNSNS}^{2+}$[12] according to which all the bonds in these cations are expected to have some π-bonding character. The π-bond orders estimated from the bond distances in $\overline{SeNSNS}^{2+}$ (see Table 8) and $\overline{SeNSNS}^{\bullet+}$ (see Fig. 5) indicate the presence of thermodynamically stable delocalised $3p_\pi(S)$–$2p_\pi(N)$ and $4p_\pi(Se)$–$2p_\pi(N)$ bonds. However, the calculated Se–S bond orders are very much lower than expected on the basis of the MO treatment which indicates a substantial $4p_\pi(Se)$–$3p_\pi(S)$

* The bond order (N) was calculated by the Pauling equation: $N = 10^{(D-R)/0.71}$, where R is the observed bond length (Å) and D the sum of the appropriate covalent radii (Å) for a single bond; D = 2.21, 1.87 and 1.74 for Se–S, Se–N and S–N, respectively (see ref. 28).

Table 4 Crystallographic data for $\overline{SeNSNS}(AsF_6)_2$[a] **1**, $(\overline{SeNSNS})_2(AsF_6)_2$[b] **2**, $(Se/\overline{SNSNSe})_2(AsF_6)_2$[c] **3** and $Cl\overline{SeNSNS}AsF_6$ **4**

Compound	1	2	3	4
Formula	$As_2F_{12}N_2S_2Se$	$As_2F_{12}N_4S_4Se_2$	$As_2F_{12}N_4S_3Se_3$	$AsClF_6S_2Se$
M	548.85	719.89	766.91	395.32
Crystal size/mm	0.20 × 0.20 × 0.30	0.15 × 0.20 × 0.25	0.44 × 0.30 × 0.30	0.52 × 0.37 × 0.18
System	Monoclinic	Monoclinic	Monoclinic	Monoclinic
Space group	$C2$	$P2_1/n$	$P2_1/n$	$P2_1/n$
a/Å	12.616(2)	9.768(1)	10.252(1)	9.211(1)
b/Å	8.581(2)	16.022(3)	15.995(2)	19.563(2)
c/Å	10.616(2)	10.269(1)	9.759(1)	10.600(2)
β/°	93.33(1)	97.77(1)	97.81(8)	104.93(1)
U/Å^3	1147.3(2)	1592.4(3)	1585.5(3)	1045.59
Z (molecules per cell)	4	4	4	8
D_c/Mg m^{-3}	3.177	3.003	3.21	2.85
F(000)	1016.0	1336.0	1408	1472
μ(Mo-Kα)/mm^{-1}	944.5	933.6	11.53	8.36
No. of reflections	1150	2962	2781	4887
No. of unique reflections	1002	2210	2781	2387
Observed reflections	940[d]	1459[d]	2143[e]	1589[e]
R_f[f] obs.	0.041	0.046	0.062	0.043
(all)			0.086	0.080
R'[g] obs.	0.046	0.0519	0.087	0.080
(all)			0.090	0.055

[a] Occupancy factors: S, 0.51; Se, 0.49. [b] Occupancy factors: Se(1) 0.70, S(11′) 0.30, S(11) 0.70, Se(1′) 0.30, S(21) 0.65, Se(2′) 0.35, Se(2) 0.65, S(21′) 0.35. [c] Occupancy factors: S 0.50, Se 0.50. [d] $I_{net} > 3\sigma I_{net}$. [e] $I_{net} > 2.5\sigma I_{net}$. [f] $R_f = \Sigma||F_o| - |F_c||/\Sigma|F_o|$. [g] $R' = [\Sigma w(|F_o| - |F_c|)^2/\Sigma w|F_o|]^{\frac{1}{2}}$, where $w = 1/\sigma^2 I$.

Table 5 Fractional atomic coordinates with estimated standard deviations (e.s.d.s) in parentheses

Atom	X/a	Y/b	Z/c
$(Se/\overline{SNSNS}/Se)_2(AsF_6)_2$			
As(1)	0.2482(1)	0.1539(1)	0.1367(1)
F(11)	0.1654(9)	0.0942(5)	0.0113(8)
F(12)	0.3194(9)	0.2170(5)	0.2643(7)
F(13)	0.093(1)	0.176(1)	0.180(1)
F(14)	0.400(1)	0.137(1)	0.091(2)
F(15)	0.210(2)	0.2380(6)	0.039(1)
F(16)	0.265(1)	0.0736(5)	0.243(1)
As(2)	0.2644(1)	−0.0586(9)	0.6926(1)
F(21)	0.245(1)	0.0107(6)	0.5647(8)
F(22)	0.2851(8)	−0.1278(5)	0.8223(7)
F(23)	0.1333(9)	−0.0147(6)	0.7589(9)
F(24)	0.3917(8)	−0.1067(6)	0.6293(9)
F(25)	0.1538(8)	−0.1266(5)	0.6090(8)
F(26)	0.375(1)	0.0077(6)	0.780(1)
Se(1)	0.3622(7)	0.2047(6)	0.5358(6)
S(11)	0.131(3)	0.195(2)	0.472(2)
S(11′)	0.355(5)	0.197(2)	0.538(3)
Se(1′)	0.125(3)	0.1966(1)	0.468(2)
S(12)	0.1977(3)	0.1905(2)	0.7449(3)
N(11)	0.345(1)	0.1991(6)	0.7010(9)
N(12)	0.087(1)	0.1886(7)	0.625(1)
Se(2)	0.6230(8)	0.1154(2)	0.9025(7)
S(21)	0.853(2)	0.1073(1)	0.967(2)
S(21′)	0.625(4)	0.1008(1)	0.898(3)
Se(2′)	0.856(1)	0.1106(8)	0.967(1)
S(22)	0.7852(3)	0.1010(2)	0.6920(3)
N(21)	0.637(1)	0.1062(6)	0.734(1)
N(22)	0.901(1)	0.1017(6)	0.816(1)

Atom	X/a	Y/b	Z/c
$Se/\overline{SNSNS}/Se(AsF_6)_2$			
Se(1)	−0.2083(4)	−0.9718(4)	−0.1481(5)
S(2)	−0.211(1)	−0.948(1)	−0.359(1)
S(1′)	−0.200(1)	−0.943(1)	−0.145(1)
Se(2′)	−0.2156(5)	−0.9780(4)	−0.3542(5)
S(3)	−0.1486(2)	−0.6769(3)	−0.2569(3)
N(1)	−0.1688(8)	−0.779(1)	−0.1354(9)
N(2)	−0.1769(7)	−0.786(1)	−0.3730(8)
As(1)	−0.8646(1)	−0.8497(0)	−0.2514(1)
F(11)	−0.8062(7)	−0.967(1)	−0.1372(7)
F(12)	−0.9172(8)	−0.722(1)	−0.3639(9)
F(13)	−0.9766(7)	−0.951(1)	−0.257(1)
F(14)	−0.8118(7)	−0.970(1)	−0.3596(8)
F(15)	−0.7497(9)	−0.742(1)	−0.247(1)
F(16)	−0.912(1)	−0.735(1)	−0.137(1)
As(2)	0.0000(0)	−0.3330(2)	−0.5000(0)
F(21)	−0.0781(8)	−0.474(1)	−0.4447(9)
F(22)	−0.0794(8)	−0.191(1)	−0.4428(9)
F(23)	0.0772(7)	−0.333(1)	−0.3627(7)
As(3)	0.000(0)	−0.3269(2)	−0.0000(0)
F(31)	−0.056(1)	−0.460(1)	−0.097(1)
F(32)	0.1100(8)	−0.316(1)	−0.082(1)
F(33)	−0.0529(9)	−0.187(1)	−0.096(1)

contribution from the totally symmetric bonding MO in the Se–S region. Similar unexpected long chalcogen–chalcogen bonds are also observed in the related $Se_{3-x}S_xN_2^{n+}$ (x = 0, 1 or 3; n = 1 or 2).[3,12,14]

The error in the structural determination is illustrated by the high estimated standard deviations particularly in the NSeNS moiety and by the fact that the S–N bond [1.77(4) Å] adjacent to the Se–S bond in the bottom ring of dimer 2 (see Fig. 5) is longer than the Se–N bond [1.66(2) Å]. In addition, the vibrational frequencies of $\overline{SeNSNS}(AsF_6)_2$ which were calculated from the average of the bond distances of $\overline{SNSNS}^{2+}$,[12] $\overline{SeNSNSe}^{2+}$[3] and $\overline{SeNSeNSe}^{2+}$[14] agreed better with the observed values than those calculated from the bond lengths obtained from the crystal structures (see Experimental section and Tables 2 and 3). Nevertheless the crystal structures of $(Se/\overline{SNSNS}/Se^{\bullet+})_2$ and $Se/\overline{SNSNS}/Se^{2+}$ establish the identities of the compounds. The Se–S and the adjacent S–N bonds in $\overline{SeNSNS}^{2+}$ are shorter than those in $\overline{SeNSNS}^{\bullet+}$ whereas the Se–N and the S–N (of the NSN fragment) bonds in the two cations are essentially the same (see Figs. 5 and 7). The changes in the bond distances which accompany the oxidation

Table 6 Fractional atomic and positional parameters with e.s.d.s in parentheses

Atom	*X/a*	*Y/b*	*Z/c*
$(Se/\overline{SNSNSe})_2(AsF_6)_2$			
Se(11)	0.401 8(2)	0.112 6(1)	0.623 1(2)
S/S(12)	0.467 6(2)	0.108 8(1)	0.855 1(2)
N(13)	0.314(1)	0.101 6(7)	0.899(1)
S(14)	0.192 9(4)	0.101 1(2)	0.785 9(4)
N(15)	0.235(1)	0.107(7)	0.640(1)
Se(21)	0.535 7(2)	0.296 3(1)	0.861 3(2)
Se/S(22)	0.469 8(2)	0.304 0(2)	0.628 0(2)
N(23)	0.622(1)	0.311 3(7)	0.586(1)
S(24)	0.744 7(4)	0.309 4(2)	0.697 8(4)
N(25)	0.703(1)	0.302 7(7)	0.844(1)
As(1)	0.136 5(1)	0.346 16(8)	0.748 2(2)
F(11)	0.012 5(9)	0.406 8(6)	0.669(1)
F(12)	0.263 8(9)	0.282 7(6)	0.820(1)
F(13)	0.086(2)	0.360(1)	0.898(1)
F(14)	0.041(1)	0.262 8(8)	0.716(3)
F(15)	0.186(1)	0.324(1)	0.594(1)
F(16)	0.243(1)	0.426 6(6)	0.763(2)
As(2)	0.192 4(1)	0.941 45(9)	0.264 3(2)
F(21)	0.325 7(8)	0.871 8(5)	0.286 9(9)
F(22)	0.283(1)	1.007 7(7)	0.376(1)
F(23)	0.129(1)	0.893 0(7)	0.394(1)
F(24)	0.066(1)	1.011 2(7)	0.244(1)
F(25)	0.108 8(9)	0.872 1(6)	0.150 7(9)
F(26)	0.259(1)	0.988 1(7)	0.135(1)

Atom	*X/a*	*Y/b*	*Z/c*
$ClSeNSNSAsF_6$			
Se(1)	0.366 6(1)	0.221 41(7)	0.971 3(1)
Cl(1)	0.570 8(4)	0.161 0(2)	1.040 7(4)
S(11)	0.367 6(4)	0.234 8(2)	0.758 6(3)
S(12)	0.463 7(4)	0.351 1(2)	0.901 3(4)
N(11)	0.432(1)	0.310 8(6)	0.773(1)
N(12)	0.423(1)	0.306 3(5)	1.010 1(9)
Se(2)	0.185 1(1)	0.516 36(7)	0.323 5(1)
Cl(2)	0.372 9(4)	0.585 5(2)	0.401 4(3)
S(21)	0.196 8(4)	0.507 9(2)	0.112 4(3)
S(22)	0.321 4(4)	0.395 8(2)	0.253 9(4)
N(21)	0.282(1)	0.436 5(6)	0.126(1)
N(22)	0.260(1)	0.433 0(5)	0.361 5(9)
As(1)	0.431 3(1)	0.208 03(7)	0.399 3(1)
F(11)	0.422(1)	0.285 5(5)	0.464(1)
F(12)	0.288(1)	0.182 9(6)	0.458(1)
F(13)	0.550(1)	0.184 3(5)	0.539(1)
F(14)	0.313(1)	0.230 4(5)	0.257 8(9)
F(15)	0.573(1)	0.231 8(7)	0.342(1)
F(16)	0.437(1)	0.130 5(5)	0.335(1)
As(2)	0.749 1(1)	0.965 41(6)	0.248 2(1)
F(21)	0.902 3(9)	0.998 2(5)	0.216 1(9)
F(22)	0.645 6(9)	0.984 8(5)	0.096 8(7)
F(23)	0.788(1)	0.889 3(4)	0.193 0(9)
F(24)	0.702(1)	1.040 0(5)	0.303 2(9)
F(25)	0.848 5(9)	0.943 8(6)	0.399 1(7)
F(26)	0.592 7(8)	0.932 3(5)	0.278 0(9)

Table 7 Bond distances (Å)* in the AsF_6^- and angles (°) in $(Se/\overline{SNSNS}/Se^{\bullet+})_2$ with e.s.d.s in parentheses

As(1)–F(11)	1.700(8)	As(2)–F(21)	1.720(9)
As(1)–F(12)	1.725(8)	As(2)–F(22)	1.733(7)
As(1)–F(13)	1.66(1)	As(2)–F(23)	1.687(9)
As(1)–F(14)	1.61(2)	As(2)–F(24)	1.671(9)
As(1)–F(15)	1.66(1)	As(2)–F(25)	1.699(8)
As(1)–F(16)	1.67(1)	As(2)–F(26)	1.69(1)
S(11)–Se(1)–N(11)	93.3(7)	N(21)–S(22)–N(22)	111.2(5)
Se(1)–S(11)–N(12)	96(1)	Se(1)–N(11)–S(12)	119.0(6)
Se(1')–S(11')–N(11)	97(2)	S(11')–N(11)–S(12)	117(1)
S(11')–Se(1')–N(12)	93(1)	S(11)–N(12)–S(12)	120(1)
N(11)–S(12)–N(12)	110.6(5)	Se(1')–N(12)–S(12)	121(1)
S(21)–Se(2)–N(21)	95.2(7)	Se(2)–N(21)–S(22)	118.3(7)
Se(2)–S(21)–N(22)	95.9(9)	S(21')–N(21)–S(22)	117.2(2)
Se(2')–S(21')–N(21)	94(2)	S(21)–N(22)–S(22)	119.4(9)
S(21)–Se(2')–N(22)	95(1)	Se(2')–N(22)–S(22)	121.2(8)

* Bond distances within the $(Se/\overline{SNSNS}/Se^{\bullet+})_2$ cation are included in Fig. 5. Occupancy factors of the disordered atoms are: Se(1) 0.70, S(11') 0.30, S(11) 0.70, Se(1') 0.30, S(21) 0.65, Se(2') 0.35, Se(2) 0.65, S(21') 0.35.

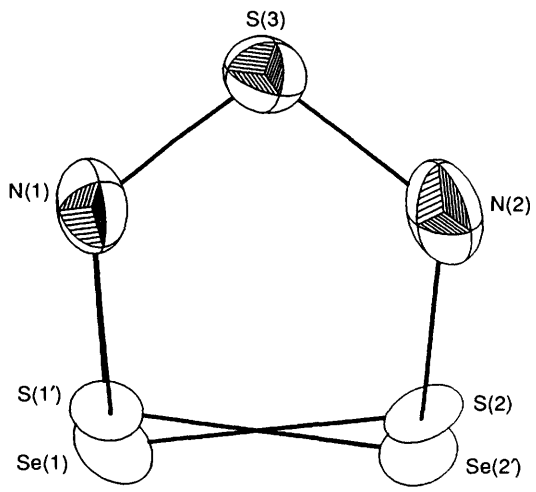

Fig. 6 An ORTEP plot of the disordered $Se/\overline{SNSNS}/Se^{2+}$. Occupancy factors: Se(1), S(2) 0.51; S(1'), Se(2') 0.49

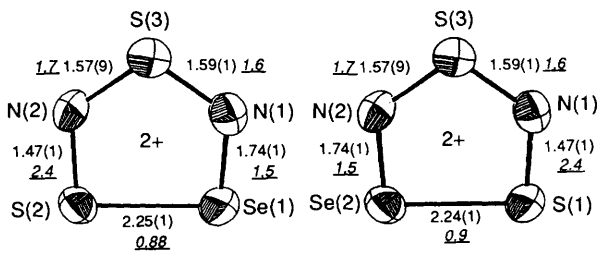

Fig. 7 Bond distances (Å) and calculated bond orders (italics underlined) in the two independent $\overline{SeNSNS}^{2+}$ cations

of $\overline{SeNSNS}^{\bullet+}$ to $\overline{SeNSNS}^{2+}$ are therefore somewhat consistent with the nature of the SOMO of $\overline{SeNSNS}^{\bullet+}$ assuming it is the same as that of $\overline{SNSNS}^{\bullet+}$. Similar changes in bond distances are observed in the related $Se_{3-x}S_xN_2^{\bullet+}$–$Se_{3-x}S_xN_2^{2+}$ (x = 0, 1 or 3)[3,12,14] monocation–dication systems. The Se–S bonds in both $(Se/\overline{SNSNS}/Se^{\bullet+})_2$ and $Se/\overline{SNSNS}/Se^{2+}$ are intermediate between the corresponding S–S and Se–Se distances in $\overline{SNSNS}^{n+}$ [12,30] and $\overline{SeNSNSe}^{n+}$ [3,29] (n = 1 or 2) as expected.

The crystal structure of $(Se/\overline{SNSNSe})_2(AsF_6)_2$ consists of disordered $\overline{SeNSNSe}^{\bullet+}$ and $\overline{SeNSNS}^{\bullet+}$ radical cations joined by two long Se/S · · · Se bonds [3.077(3), 3.138(3) Å] as shown in Fig. 8. In this structure one atomic position was fitted by 50% sulfur and 50% selenium and no attempt was made to unravel the disorder. The structure is centrosymmetric with a geometry similar to those of related dimers (see above). The bond distances and angles in $(Se/\overline{SNSNSe}^{\bullet+})_2$ are essentially the same as those in $(\overline{SeNSNSe}^{\bullet+})_2$[29] (see Tables 9 and 10; angles in the latter cation are not included). The Se/S–Se and Se/S–N bonds in $(Se/\overline{SNSNSe}^{\bullet+})_2$ have values expected upon superimposition

Table 8 Bond distances (Å) * and angles (°) for Se/$\overline{SNSNS}$/Se$(AsF_6)_2$ with e.s.d.s in parentheses

Se(1)–S(2)	2.25(1)	S(2)–Se(1)–N(1)	88.9(5)
Se(1)–N(1)	1.74(1)	Se(1)–S(2)–N(2)	101.2(6)
S(2)–N(2)	1.47(1)	Se(2')–S(1')–N(1)	102.1(7)
S(1')–Se(2')	2.24(1)	S(1')–Se(2')–N(2)	88.6(4)
S(1')–N(1)	1.47(1)	N(1)–S(3)–N(2)	105.7(5)
Se(2')–N(2)	1.74(1)	Se(1)–N(1)–S(3)	121.3(6)
S(3)–N(1)	1.59(1)	Se(1')–N(1)–S(3)	121.6(8)
S(3)–N(2)	1.57(9)	S(2)–N(2)–S(3)	122.8(7)
		S(2')–N(2)–S(3)	121.8(6)
As(1)–F(11)	1.709(9)	As(2)–F(21)	1.69(1)
As(1)–F(12)	1.72(1)	As(2)–F(22)	1.71(1)
As(1)–F(13)	1.66(1)	As(2)–F(23)	1.705(9)
As(1)–F(14)	1.705(9)	As(3)–F(31)	1.67(1)
As(1)–F(15)	1.72(1)	As(3)–F(32)	1.69(1)
As(1)–F(16)	1.70(1)	As(3)–F(33)	1.69(1)

* Atoms S(1') and Se(2') are the disordered pair of Se(1) and S(2); they have an occupancy factor of 0.490(4).

Table 9 Comparison of bond distances (Å) in the $(Se/\overline{SNSNSe}^{\bullet+})_2$ and $(\overline{SeNSNSe}^{\bullet+})_2$ cations with e.s.d.s in parentheses

$(Se/\overline{SNSNSe}^{\bullet+})_2$ [a]		$(\overline{SeNSNSe}^{\bullet+})_2$ [b]	
Se/S(22)–Se(21)	2.288(3)	Se(1)–Se(2)	2.358(2)
Se(11)–Se/S(12)	2.274(3)	Se(3)–Se(4)	2.345(2)
Se(21)–N(25)	1.75(1)	Se(1)–N(1)	1.75(1)
Se/S(22)–N(23)	1.67(1)	Se(2)–N(2)	1.75(1)
Se(11)–N(15)	1.74(1)	Se(3)–N(3)	1.76(1)
Se/S(12)–N(13)	1.69(1)	Se(4)–N(4)	1.76(1)
S(24)–N(25)	1.55(1)	S(1)–N(1)	1.55(1)
S(24)–N(23)	1.55(1)	S(1)–N(2)	1.57(1)
S(14)–N(13)	1.54(1)	S(2)–N(4)	1.54(1)
S(14)–N(15)	1.55(1)	S(2)–N(3)	1.58(1)
Se(21) · · · Se/S(12)	3.077(3)	Se(1) · · · Se(4)	3.159(2)
Se/S(22) · · · Se(11)	3.138(3)	Se(2) · · · Se(3)	3.111(2)
AsF_6^- in $(Se/\overline{SNSNSe}^{\bullet+})_2$			
As(1)–F(11)	1.700(8)	As(2)–F(21)	1.753(8)
As(1)–F(12)	1.725(9)	As(2)–F(22)	1.704(9)
As(1)–F(13)	1.63(1)	As(2)–F(23)	1.684(9)
As(1)–F(14)	1.66(1)	As(2)–F(24)	1.702(9)
As(1)–F(15)	1.69(1)	As(2)–F(25)	1.714(8)
As(1)–F(16)	1.68(1)	As(2)–F(26)	1.685(9)

[a] This work; Se/S denotes 50% occupancy by S and Se. [b] Ref. 29.

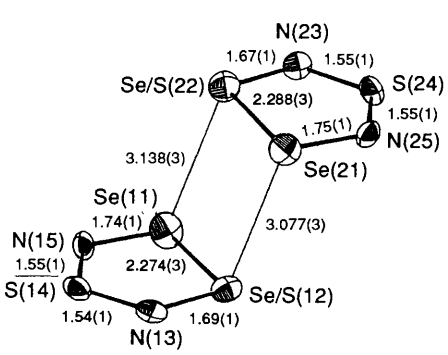

Fig. 8 An ORTEP plot of the disordered $(Se/\overline{SNSNSe}^{\bullet+})_2$ with bond distances (Å). Se/S denotes 50% occupancy by S and Se

of the Se–Se (or Se–N) bond in $(\overline{SeNSNSe}^{\bullet+})_2$ [29] and the S–S (or S–N) bond in $(\overline{SNSNS}^{\bullet+})_2$.[30]

Crystal Structure of $ClSeNSNSAsF_6$.—The X-ray crystal structure of $ClSeNSNSAsF_6$ consists of two independent $ClSeNSNS^+$ cations and AsF_6^- anions. The five-membered rings are almost planar and the Se atoms in the two independent cations deviate from the planes formed by the S_2N_2 moiety by 0.12(1) and 0.19(1) Å. The bond distances in the two cations are similar to those in $ClSeNSNS^+X^-$ (X = Cl[9] or $AlCl_4$ [25b]) with some differences in the Se–S bond in the $AlCl_4^-$ and the Se–Cl bond in the Cl^- salts, both of which are significantly longer than the corresponding distances in the other two salts (see Table 11). The structures of $ClSeNSNS^+X^-$ (X = Cl or $AlCl_4$) have already been discussed in detail, therefore a discussion of that in $ClSeNSNSAsF_6$ is not warranted.

Table 10 Bond angles (°) in $(Se/\overline{SNSNSe})_2(AsF_6)_2$ with e.s.d.s in parentheses

N(25)–Se(21)–Se/S(22)	93.6(4)	S(14)–N(13)–Se/S(12)	120.4(7)
N(23)–Se/S(22)–Se(21)	95.0(4)	Se/S(12)–Se(21)–Se/S(22)	89.83(9)
N(25)–S(24)–N(23)	110.5(6)	N(25)–Se(21)–Se/S(12)	106.1(4)
S(24)–N(25)–Se(21)	119.3(7)	Se(21)–Se/S(22)–Se(11)	89.89(9)
S(24)–N(23)–Se/S(22)	121.6(7)	N(23)–Se/S(22)–Se(11)	106.1(4)
N(15)–Se(11)–Se/S(12)	93.8(4)	Se/S(12)–Se(11)–Se/S(22)	88.57(9)
N(13)–Se/S(12)–Se(11)	95.3(4)	N(15)–Se(11)–Se/S(22)	105.5(4)
N(15)–S(14)–N(13)	111.1(6)	Se(11)–Se/S(12)–Se(21)	91.7(9)
S(14)–N(15)–Se(11)	119.4(7)	N(13)–Se/S(12)–Se(21)	106.1(4)

Table 11 Comparison of bond lengths (Å) and angles (°) in $ClSeNSNSX$

	X			
	AsF_6^- [a]		$AlCl_4^-$ [b]	Cl^- [c]
Se(1)–S(11)	2.272(4)	[2.273(3)] [d]	2.293(1)	2.277(2)
S(11)–N(11)	1.59(1)	[1.59(1)]	1.630(4)	1.653(7)
N(11)–S(12)	1.53(1)	[1.54(1)]	1.545(4)	1.569(8)
S(12)–N(12)	1.57(1)	[1.58(1)]	1.578(4)	1.561(6)
N(12)–Se(1)	1.76(1)	[1.78(1)]	1.741(4)	1.788(7)
Se(1)–Cl(1)	2.182(4)	[2.183(3)]	2.191(1)	2.249(3)
As(1)–F(11)	1.676(9)			
As(1)–F(12)	1.675(9)			
As(1)–F(13)	1.661(9)			
As(1)–F(14)	1.668(8)			
As(1)–F(15)	1.647(9)			
As(1)–F(16)	1.670(9)			
As(2)–F(21)	1.664(8)			
As(2)–F(22)	1.686(7)			
As(2)–F(23)	1.671(8)			
As(2)–F(24)	1.669(9)			
As(2)–F(25)	1.680(7)			
As(2)–F(26)	1.682(8)			
S(11)–Se(1)–Cl(1)	100.0(2)	[100.5(1)] [d]	101.46(5)	98.29(9)
N(12)–Se(1)–Cl(1)	104.8(3)	[105.1(3)]	103.7(1)	100.4(2)
N(12)–Se(1)–S(11)	92.7(3)	[92.5(3)]	92.7(1)	92.9(2)
Se(1)–S(11)–N(11)	96.2(4)	[97.1(4)]	96.1(1)	97.2(2)
S(11)–N(11)–S(12)	123.3(7)	[122.1(7)]	121.6(2)	120.4(4)
N(11)–S(12)–N(12)	109.6(6)	[108.8(6)]	110.2(2)	110.0(4)
S(12)–N(12)–Se(1)	118.0(6)	[116.7(6)]	118.6(2)	118.3(4)

[a] This work. [b] Ref. 25. [c] Ref. 9. [d] The second value given in each case corresponds to that for the other independent cation.

Conclusion

Our attempts to prepare $SeNSAsF_6$ led instead to the synthesis of $\overline{SeNSNS}(AsF_6)_2$ and $(\overline{SeNSNS})_2(AsF_6)_2$ and the completion of the preparation and characterisation of all possible 7π $Se_{3-x}S_xN_2^{\bullet+}$ and 6π $Se_{3-x}S_xN_2^{2+}$ (x = 1–3) ring systems in solution and the solid state. The first cation of this class $\overline{SNSNS}^{\bullet+}$ was first identified in 1974 by Banister *et al.*[33] in their seminal paper on $(\overline{SNSNS})_2(S_2O_6Cl)_2$. Later Gillespie *et al.*[29] characterised $\overline{SeNSNSe}^{\bullet+}$ in $(\overline{SeNSNSe})_2(AsF_6)_2$ and since then we have

prepared and structurally characterised $\overline{SeNSNSe}(AsF_6)_2$,[3,34] $\overline{SNSNS}(AsF_6)_2$,[12] $(\overline{SeNSeNSe})_n(AsF_6)_2$ (n = 1 or 2)[14] and $(\overline{SNSNSe})_n(AsF_6)_2$ (n = 1 or 2; this report). However, the isomers $\overline{SNSeNS}^{n+}$ and $\overline{SeNSeNS}^{n+}$ (n = 1 or 2) have not been identified. Although $SNSe^+$ has not been isolated, it is proposed as a reaction intermediate. In contrast to $\overline{SNSNS}^{2+}$, which completely dissociates to SNS^+ and SN^+ in SO_2 and AsF_3 solution, all the selenium-containing analogues retain their ring structures in solution.

Acknowledgements

We thank Dr. J. L. Howe (Bruker Canada Ltd.) for Fourier-Transform Raman spectra and Dr. L. Calhoun (University of New Brunswick) for assistance in obtaining multinuclear NMR spectra. We also thank Natural Sciences and Engineering Research Council (Canada) and the University of New Brunswick (E. G. A. and X. S.) for financial support.

References

1 E. G. Awere and J. Passmore, *J. Chem. Soc., Dalton Trans.*, 1992, 1343.
2 W. V. F. Brooks, G. K. MacLean, J. Passmore, P. S. White, and C.-M. Wong, *J. Chem. Soc., Dalton Trans.*, 1983, 1961; G. K. McLean, J. Passmore and P. S. White, *J. Chem. Soc., Dalton Trans.*, 1984, 211; G. K. MacLean, J. Passmore, M. N. S. Rao, M. J. Schriver and P. S. White, *J. Chem. Soc., Dalton Trans.*, 1985, 1405; E. G. Awere, N. Burford, C. Mailer, J. Passmore, M. J. Schriver, P. S. White, A. J. Banister, H. Oberhammer and L. H. Sutcliffe, *J. Chem. Soc., Chem. Commun.*, 1987, 66; N. Burford, J. Passmore and M. J. Schriver, *J. Chem. Soc., Chem. Commun.*, 1986, 140; N. Burford, J. P. Johnson, J. Passmore, M. J. Schriver and P. S. White, *J. Chem. Soc., Chem. Commun.*, 1986, 966; M. J. Schriver, Ph.D. Thesis, University of New Brunswick, 1988; S. Parsons, J. Passmore, M. J. Schriver and P. S. White, *J. Chem. Soc., Chem. Commun.*, 1991, 369; S. Parsons, J. Passmore, M. J. Schriver and X. Sun, *Inorg. Chem.*, 1991, **30**, 3342; A. J. Banister, J. M. Rawson, W. Clegg and S. L. Birkby, *J. Chem. Soc., Dalton Trans.*, 1991, 1099.
3 E. G. Awere, J. Passmore and P. S. White, *J. Chem. Soc., Dalton Trans.*, 1992, 1267.
4 A. Apblett, A. J. Banister, D. Biron, A. G. Kendrick, J. Passmore, M. J. Schriver and M. Stojanac, *Inorg. Chem.*, 1986, **25**, 4451.
5 (*a*) M. J. Collins, R. J. Gillespie, J. F. Sawyer and G. J. Schrobilgen, *Inorg. Chem.*, 1986, **25**, 2053; (*b*) R. C. Burns and R. J. Gillespie, *Inorg. Chem.*, 1982, **21**, 3877; (*c*) R. C. Burns, M. J. Collins, R. J. Gillespie and G. J. Schrobilgen, *Inorg. Chem.*, 1986, **25**, 4465.
6 M. P. Murchie, J. Passmore, G. W. Sutherland and R. Kapoor, *J. Chem. Soc., Dalton Trans.*, 1992, 503 and refs. therein.
7 W. A. S. Nandana, J. Passmore, P. S. White and C.-M. Wong, *Inorg. Chem.*, 1989, **28**, 3320.
8 P. A. G. O'Hare, E. G. Awere, S. Parsons and J. Passmore, *J. Chem. Thermodyn.*, 1989, **21**, 153.
9 R. J. Gillespie, J. P. Kent and J. F. Sawyer, *Inorg. Chem.*, 1990, **29**, 1251.
10 G. M. Begum and A. C. Rutenberg, *Inorg. Chem.*, 1967, **6**, 2212.
11 E. Awere, J. Passmore, K. F. Preston and L. H. Sutcliffe, *Can. J. Chem.*, 1988, **66**, 1776.
12 W. V. F. Brooks, T. S. Cameron, F. Grein, S. Parsons, J. Passmore and M. J. Schriver, *J. Chem. Soc., Chem. Commun.*, 1991, 1079; *Inorg. Chem.*, submitted for publication.
13 R. M. Badger, *J. Chem. Phys.*, 1934, **2**, 128.
14 E. G. Awere, J. Passmore, P. S. White and T. Klapötke, *J. Chem. Soc., Chem. Commun.*, 1989, 1415; E. G. Awere, J. Passmore and P. S. White, *J. Chem. Soc., Dalton Trans.*, 1993, 299.
15 T. S. Cameron and R. E. Cordes, *Acta Crystallogr., Sect. B*, 1979, **35**, 748.
16 N. Walker and D. Stuart, *Acta Crystallogr., Sect. A*, 1983, **39**, 158.
17 G. M. Sheldrick, in *Crystallographic Computing 3*, eds. G. M. Sheldrick, C. Kruger and R. Goddard, Oxford University Press, 1985, p. 175.
18 G. M. Sheldrick, SHELX 76, A system of computer programs for X-ray structure determination as locally implemented at Dalhousie and Cambridge Universities, 1976.
19 J. R. Carruthers and D. J. Watkin, CRYSTALS, Issue 8, Chemical Crystallography Laboratory, Oxford, 1989.
20 D. J. Watkin, *Crystallographic Computing 4*, eds. N. W. Isaacs and M. R. Taylor, Oxford University Press, 1983, pp. 113–125 and refs. therein.
21 V. Medizadeh and S. Mardix, *Acta Crystallogr., Sect. C*, 1986, **42**, 518.
22 Y. Le Page, P. S. White and E. J. Gabe, NRCCAD, An Enhanced CAD-4 Control Program, Annual Meeting of American Crystallographic Association, Hamilton, Ontario, 1986.
23 E. J. Gabe, Y. Le Page, J.-P. Charland and F. L. Lee, *J. Appl. Crystallogr.*, 1989, **22**, 384.
24 *International Tables for X-Ray Crystallography*, Kynoch Press, Birmingham, 1974, vol. 4.
25 (*a*) A. Apblett, F. Grein, J. P. Johnson, J. Passmore and P. S. White, *Inorg. Chem.*, 1986, **25**, 422; (*b*) A. Apblett, T. Chivers and J. F. Fait, *Inorg. Chem.*, 1990, **29**, 1643.
26 J. Passmore and M. J. Schriver, *Inorg. Chem.*, 1988, **27**, 2749.
27 C. K. Johnson, ORTEP, A Fortran Thermal Ellipsoid Plot Program, Technical Report, ORNL-5138, Oak Ridge, TN, 1976.
28 L. Pauling, *The Nature of the Chemical Bond*, 3rd edn., Cornell University, Ithaca, NY, 1960.
29 R. J. Gillespie, J. P. Kent and J. F. Sawyer, *Inorg. Chem.*, 1981, **20**, 4053.
30 R. J. Gillespie, J. P. Kent and J. F. Sawyer, *Inorg. Chem.*, 1981, **20**, 3784.
31 G. Wolmershauser and G. Heckmann, *Angew. Chem., Int. Ed. Engl.*, 1992, **31**, 779.
32 R. T. Oakley, R. W. Reed, A. Wallace Cordes, S. L. Craig and J. B. Graham, *J. Am. Chem. Soc.*, 1987, **109**, 7745.
33 A. J. Banister, H. G. Clarke, I. Rayment and H. M. M. Shearer, *Inorg. Nucl. Chem. Lett.*, 1974, **10**, 647.
34 See also A. Haas, J. Kasprowski, K. Angermund, P. Betz, Y.-H. Tsay and S. Werner, *Chem. Ber.*, 1991, **124**, 1895.

Received 30*th December* 1992; *Paper* 2/06870B